applied sciences

MDPI

Article

A Multivariate Machine Learning Model of Adsorptive Lindane Removal from Contaminated Water

Adeola Akeem Akinpelu [1], Mazen K. Nazal [1], Md Shafiullah [2,*], Md Kamrul Islam [3], Mohammed Monirul Islam [4], Aminur Rahman [4], Syed Masiur Rahman [1] and Muhammad Muhitur Rahman [3,*]

[1] Applied Research Center for Environment & Marine Studies, King Fahd University of Petroleum & Minerals (KFUPM), Dhahran 31261, Saudi Arabia; abdulhakeem@kfupm.edu.sa (A.A.A.); mazennazal@kfupm.edu.sa (M.K.N.); smrahman@kfupm.edu.sa (S.M.R.)
[2] Interdisciplinary Research Center for Renewable Energy and Power Systems, King Fahd University of Petroleum & Minerals, Dhahran 31261, Saudi Arabia
[3] Department of Civil and Environmental Engineering, College of Engineering, King Faisal University, Al-Ahsa 31982, Saudi Arabia; maislam@kfu.edu.sa
[4] Department of Biomedical Sciences, College of Clinical Pharmacy, King Faisal University, Al-Ahsa 31982, Saudi Arabia; mislam@kfu.edu.sa (M.M.I.); marahman@kfu.edu.sa (A.R.)
* Correspondence: shafiullah@kfupm.edu.sa (M.S.); mrahman@kfu.edu.sa (M.M.R.)

Abstract: It is challenging to use conventional one-variable-at-time (OVAT) batch experiments to evaluate multivariate/inter-parametric interactions between physico-chemical variables that contribute to the adsorptive removal of contaminants. Thus, chemometric prediction approaches for multivariate calibration and analysis reveal the impact of multi-parametric variation on the process of concern. Hence, we aim to develop an artificial neural network (ANN), and stepwise regression (SR) models for multivariate calibration and analysis utilizing OVAT data prepared through experimentation. After comparing the models' performance, ANN was the superior model for this application in our work. The standard deviations (SD) between the observed and ANN-predicted values were very close. The average correlation coefficient (R^2) between observed and ANN-predicted values for the training dataset was 96.9%. This confirms the ability of our developed ANN model to forecast lindane removal accurately. The testing dataset correlation coefficients (89.9% for ANN and 67.75% for SR) demonstrated a better correlation between observed and predicted ANN values. The ANN model training and testing dataset RMSE values were 1.482 and 2.402, lower than the SR values of 4.035 and 3.890. The MAPE values for the ANN model's training and testing datasets, 0.018 and 0.031, were lower than those for the SR model. The training and testing datasets have low RSR and PBIAS values, implying model strength. The R^2 and WIA values are above 0.90 for both datasets, proving the ANN model's accuracy. Applying our developed ANN model will reduce the cost of removing inorganic and organic impurities, including lindane, and optimize chemical utilization.

Keywords: artificial neural network; contaminant removal; lindane; machine learning; multivariate stepwise regression; seagrass

check for updates

Citation: Akinpelu, A.A.; Nazal, M.K.; Shafiullah, M.; Islam, M.K.; Islam, M.M.; Rahman, A.; Rahman, S.M.; Rahman, M.M. A Multivariate Machine Learning Model of Adsorptive Lindane Removal from Contaminated Water. *Appl. Sci.* **2023**, *13*, 7086. https://doi.org/10.3390/app13127086

Academic Editor: Francisco José Alguacil

Received: 14 May 2023
Revised: 3 June 2023
Accepted: 12 June 2023
Published: 13 June 2023

Copyright: © 2023 by the authors. Licensee MDPI, Basel, Switzerland. This article is an open access article distributed under the terms and conditions of the Creative Commons Attribution (CC BY) license (https://creativecommons.org/licenses/by/4.0/).

1. Introduction

An organochlorine insecticide known as lindane (1r,2R,3S,4r,5R,6S-hexachlorocyclohexane, more commonly referred to as -HCH) has been the focus of extensive research in recent decades [1–4]. Since the 1940s, lindane has found widespread application in the fields of agricultural pest management, seed treatments, the treatment of poultry and cattle, domestic vector control, the protection of lumber, the treatment of lice and scabies, and even the treatment of rats using bait [5]. In soil, lindane is adsorbed to the soil particles, volatilized to the atmosphere, taken up by crop plants, or leached into groundwater. Even though lindane is treated, it still gets into creeks, rivers, lakes, and the ocean. Even a minimal amount of lindane

in the water is dangerous. Lindane stays in the environment for a long time, where it can get into the cells of fish and, consequently, humans. Moreover, the pesticide may lessen the motility and concentration of sperm, alter the specific activity of a testicular marker enzyme, and cause oxidative stress in humans [6]. Additionally, it may cause testicular dysgenesis syndrome, alter serum testosterone levels, and reduce the amount of testosterone in the body. The presence of a significant number of chlorine atoms within the molecule of lindane causes it to be regarded as a substance that can cause disruptions to the body's endocrine system [7]. This is because lindane is a highly toxic substance. Because of its high persistence level and ability to bioaccumulate and travel long distances, lindane is classified as a persistent organic pollutant, or POP [7]. As a result, there has been a rise in research focused on Lindane removal from contaminated water. The adsorptive removal method has been given a lot of preference in recent years because, compared to other ways, it has a very high efficiency at a low cost [8]. Adsorption, however, is controlled by several process variables, including temperature, pH of the medium, and contact time and concentration between the adsorbate and adsorbent. The impact of these parameters on the adsorption process is typically evaluated using batch adsorption studies that use the traditional OVAT approach [9]. This approach usually consumes time and resources and does not account for multivariate interactions among the variables [10]. Adsorption studies based on OVATs have challenges when examining multivariate/inter-parametric interactions between the physico-chemical parameters that synergize contaminant uptake [9]. Multivariate calibration and analysis using chemometric prediction techniques like ANN provide crucial insight into the impact of normative variability on the method in question [11].

The ANN is a tool that has recently become a powerful method for addressing issues prevalent in the real world and has garnered a great deal of attention due to its applications in various fields [12–14]. For example, it has been utilized in water treatment and offers solutions that are both practical and effective for the problem of water pollution [12]. However, the comparison of ANN and SR performances for the adsorption applications is scanty in the literature. In this work, however, we want to look at the model that will suggest optimum parameters that will give us the highest removal efficiency without rigorous experiments. These rigorous experiments consume a lot of time, energy, and cost. This is similar to the idea presented by Asadi et al. when they investigated multivariate optimization of mechanical and microstructural properties using AI tools [15].

Therefore, our interest in this work is to use the results from OVAT experiments to develop ANN and SR models that can be used for multivariate calibration and analysis. The performance of the two models was also compared, and it was confirmed that ANN was the best for this application. It is anticipated that the implementation of the developed ANN will result in a reduction of the overhead costs associated with the water treatment process. As a result of the application, the cost of removing numerous inorganic and organic pollutants in the contaminated water, such as lindane, will be reduced, and the usage of chemicals will be optimized.

The details of the developed models, adsorption experiment setup, and preliminary statistical details of the data set are described in the materials and method section of the manuscript. Subsequently, the strength of the developed predictive models based on the correlation coefficient values, root mean square error (RMSE), and mean absolute percentage error (MAPE) are compared and reported in the result section of the manuscript.

2. Materials and Methods

The proposed ANN's theoretical foundation is presented in this section. In addition to the models and simulation data, the computational methods utilized to construct them are described.

2.1. Adsorption Experiment

Experiments with an OVAT were carried out at room temperature (24 °C) using the batch process method (Figure 1), and 25 mL of Deionized water with 5% methanol was used in the experiments. Lindane was added in varying concentrations to the solutions (0.05 to

2 mg L^{-1}). The duration required to achieve equilibrium adsorption was ascertained by altering the shaking time at ambient temperature, utilizing a mass of 150 mg of adsorbent, and a rotational speed of 150 rpm, spanning a range of 5 to 5760 min. The effect of the amount of adsorbent was examined by manipulating the weight of the adsorbent within the range of 10 mg to 300 mg while keeping all other parameters unchanged. The impact of augmenting the primary Lindane level from 0.05 to 2 mg L^{-1} was examined similarly while keeping all other factors unchanged. Several standards and quality control samples were analyzed; some were blanks in which the adsorbent was present in the same solution without the adsorbate and others in which the adsorbate was present without the adsorbent. Using multiple reaction monitoring (MRM) modes on a GC-MS (GCMS TQ 8030 Shimadzu, Kyoto, Japan), we were able to calculate the concentrations of the analytes of interest. A 30 m 0.25 mm internal diameter Rxi-1 ms column with a 0.25 m film thickness was used (Restek, Bellefonte, PA, USA). The standard operating temperature for the instrument's injector was 300 °C. Highly pure helium (99.999%) was used as the carrier gas, with a flow rate of 1.87 mL/min. An injection volume of 1.0 µL was performed in splitless mode. From 70 °C, the oven temperature was raised to 200 °C at 10 °C per minute. The detector was kept at a steady 250 °C.

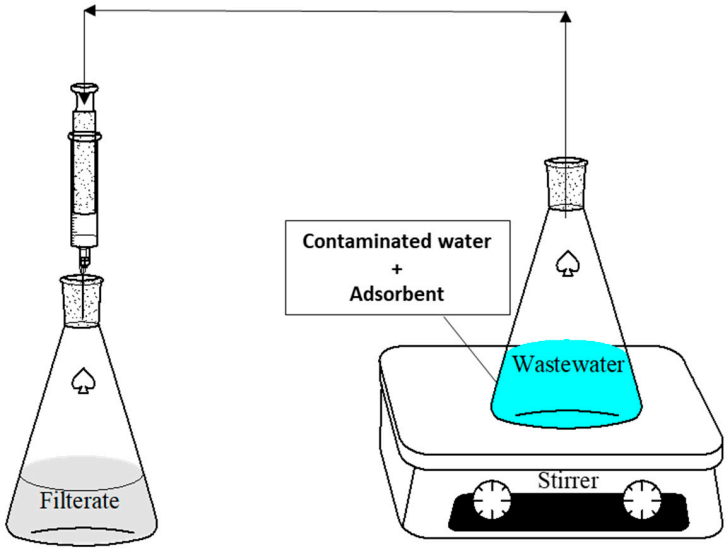

Figure 1. One-variable-at-time experimental setup.

2.2. Stepwise Linear Regression

Estimates of RA values were made using multiple stepwise regression (SR) in MATLAB (version 2019a). An onward and reverse selection was used in SR to zero in on the model's most crucial parameters. The method was proposed to overcome problems with conventional multiple regression computation [16,17]. Multiple SR analysis has become a popular and helpful method in recent years. The technique is simple, flexible, and widely applicable [18]. SR is recommended for multiple independent variables [19]. The selection of SR was based on its capacity to handle many predictor factors, exhibit high computational efficiency, enable model fine-tuning, and facilitate prompt execution [20].

In SR, two stages are involved in determining the best possible set of predictors: Step-by-step reverse removal of insignificant parameters according to predetermined limit [21] and onward choice of input parameters in a "greedy style" to reduce the remainder of the squares at every stage. In this type of calculation, two distinct value thresholds are used for introducing and dropping parameters, respectively. If the importance of any potential parameters falls below a particular limit when an additional parameter is introduced to the set of factors that predict, SR will reject the new parameter. *t*-tests and F-tests are used in SR models to incorporate or eliminate variables that predict. The ideal combination of "N" predictor parameters is achieved in the final model. The Gauss–

Jordan algorithm transforming rules, which consider the recurrent relationship among the regression coefficient, the remaining covariance variables, and the reverse of the covariance matrix's partitioning elements, provide the conceptual foundation for a stepwise regression model. Assume mode begins with a forward choice with no variable that predicts (Equation (1)) to illustrate SR's conceptual framework. Regression formulae can be completed by adding variables one at a time (Equation (2)) if they satisfy specific criteria (l F-ratio). To get rid of unnecessary predictors, sequential backward regression is performed.

$$y = \beta_0 + \varepsilon \tag{1}$$

$$y = \beta_0 + \beta_1 x_1 + \beta_2 x_2 + \ldots + \beta_n x_n + \varepsilon \tag{2}$$

In the current study, the independent variable is denoted by y, which represents the RA value. However, each of the dependent or explanatory variables, including retroreflective sheeting brand, grade, color, orientation, observation angle, age, and others, are represented by x_1, x_2, and x_n. The regression coefficients, β_0, β_1, β_2, and so on, estimate the relationship between the independent and dependent variables. Additionally, the random error is represented by ε.

2.3. Artificial Neural Networks

ANN is the most powerful computational technique for use in the fields of AI and ML right now. These computer programs, which take their cue from the individuals' intellect, are meant to simulate learning by analyzing the physical principles and reasoning underlying challenging practical problems in the same way humans do [22]. The ANN's construction, algorithm for processing, and ability to learn are all analogous to those of natural neurons in humans. Moreover, they are resilient to outside influences and can multitask, making them effective for detecting, classifying, grouping, and resolving prediction problems [23–26].

The multilayer perceptron (MLP) manifests a type of feedforward neural network (FFNN), the simplest kind of ANN. Models are built using controlled acquiring techniques in MLP neural networks (MLP-NN) by connecting input data to desired results. One or more "neurons," or "cells," can make up every "layer" of the neural processes. Weighted linkages relate the points in a specific layer to those in the following one. The data provided by each node are added together before being processed by a variety of nonlinear and biased functions. To pass on information to the following level of nodes, the result of every unit must be analyzed. This process is reiterated until reaching the output layer's nodes [27–29].

Figure 2 depicts a simple MLP-NN design, which includes k inputs, n hidden nodes, and m outputs per hidden node. Ultimately, this MLP-NN produces m outputs from k inputs, one for each output node. The connection weights (*wij*) and biases (*bij*) of the MLP-NN are trained in two stages. To begin predicting outputs, inputs are "propagated" from the nodes that are concealed to the results of the nodes using arbitrary values and biases. The difference between the former and the latter is then determined. The MLP-NN then adjusts the biases and weights utilized in the relationships to minimize the value difference in the second stage. Lastly, it ceases revising the biases and weights after a certain period or if the gap between observed and predicted outputs remains constant [30,31].

The relative strengths and weaknesses of the links among nodes are fine-tuned using a variety of methods of training in the neural system algorithm's learning processes. Among the most popular methods are gradient descent (GD), resilient propagation (RP), Levenberg–Marquardt (LM), scaled conjugate gradient (SCG), and one-step secant propagation (OSS). Each method, as seen in [32], has advantages and disadvantages regarding precision, integration, pace, space requirements, and so on. Figure 3 [32] shows how artificial neural networks employ many different compressing or stimulating processes. A few examples include the linear, logistic sigmoid, softmax, tan sigmoid, and ReLU models.

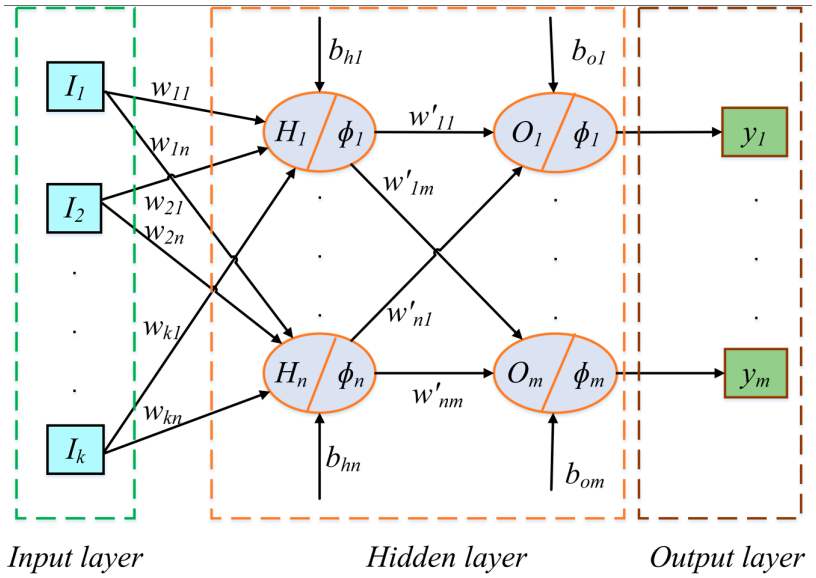

Figure 2. ANN model diagram.

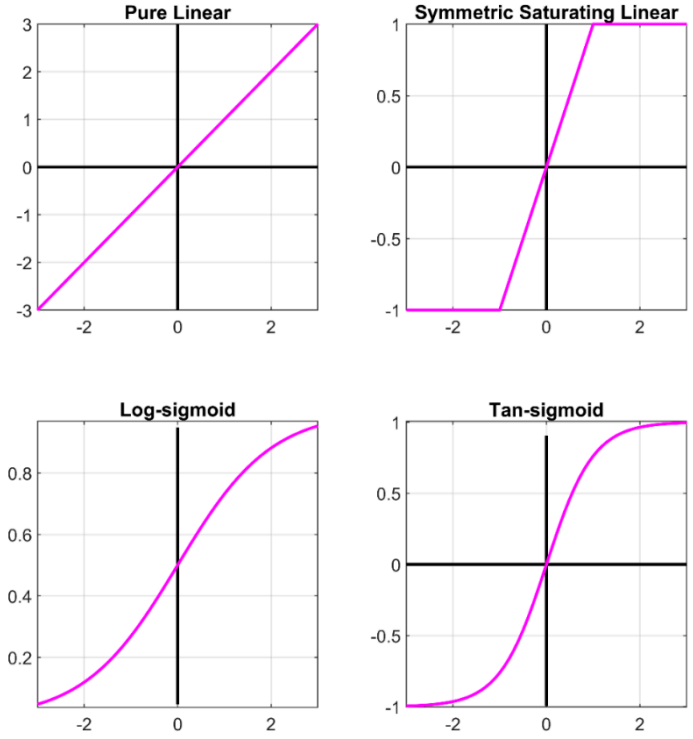

Figure 3. Squashing or activation functions.

The declining gradient issue, poor translation efficiency, overloading, and the necessity for repeated modification of the linking biases and weights are only a few of the problems plaguing traditional deep feedforward neural networks. This has led to studying numerous additional varieties of shallow neural networks [33–35]. Notable examples of such models are those based on a radial basis function (RBF), such as the extreme learning machine (ELM), the error correction model (EC), the improved second-order model (ISO), the K-nearest neighbor model (KNN), the logistic regression model (LR), the naïve Bayes model (NB), and the support vector machine (SVM).

2.4. Dataset Description

The proposed ANN model for predicting Lindane removal efficiency from contaminated water was developed from 49 datasets acquired from batch adsorption experiments. The effect of different parameters on the percentage removal of the lindane was investigated. The parameters are pH, initial concentration, temperature, contact time, and adsorbent dosage [36]. The experiments involve the adsorptive removal of lindane by seagrass powder from contaminated water. The computational tasks of the simulation and model-building processes presented in this research were performed utilizing the MATLAB computing environment. Before the developed model was put into use, the 49-dataset available for modeling was divided into two sets (training and testing sets), and 38 (77.5%) dataset was used as training. However, 22.5% of the data points (also known as the testing set) were used to test the model's performance using three performance-measuring tools. The tools are correlation coefficient (R^2), root mean square error (RMSE), and mean absolute percentage error (MAPE).

The input variables for the experiment are Dose (g), pH, Conc (mg/kg), Time (hrs), and Temp (C). However, we believe that the dataset used in this study has some limitations. The limitations involve the use of limited though common variables (5 parameters) as input to develop the models. Therefore, the model will only be valid to predict experiments that involve only these variables. Nevertheless, the limitations do not affect the performance of the model.

The data correlation matrix shows the associations between each pair of variables, and the result is presented in Figure 4. The correlation between any two input variables ranges from −0.201 to 0.676. These low values indicate that the input variables are unrelated.

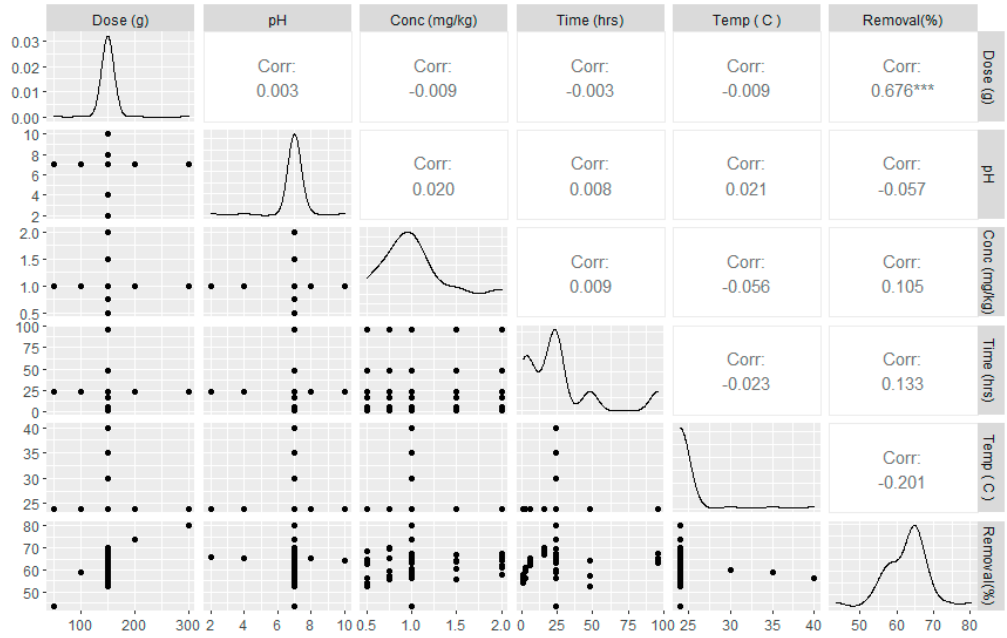

Figure 4. Statistical analysis of the raw dataset. *** symbolizes significance level at 0.01.

2.5. Computational Methodology of the Developed Model

Selected Inputs (5): Dose (g), pH, Conc (mg/kg), Time (hrs), and Temp (C).

Selected Output (1): Removal (percentage).

FFNN: Activation function: tan-sigmoid, training algorithm: backpropagation ('trainrp'); neurons in the hidden layer = 1 to 12 (4 neurons performed better than others); objective function: minimization of the MAPE of testing dataset. MATLAB function 'newff' was employed.

As reported in Table 1, the FFNNs were tested with four input variables by removing one input variable at a time for both data sets. The number of neurons in the hidden layers was kept fixed at 4. The MAPE values for each set of inputs were recorded. The higher

MAPE values in the absence of a particular input variable referred to its higher importance in the input sets and vice versa, as can be seen from the following Figure 5.

Table 1. Minimization of MAPE.

Number of Neurons	MAPE	
	Training	Testing
1	0.052535468	0.051111675
2	0.051537307	0.050463394
3	0.048195353	0.050449361
4	0.021337861	0.031621683
5	0.023813819	0.048887605
6	0.016572092	0.053637026
7	0.016127481	0.036106327
8	0.01671685	0.046555818
9	0.015428085	0.04684183
10	0.010350745	0.050320977
11	0.009477217	0.032474059
12	0.011147193	0.034483183

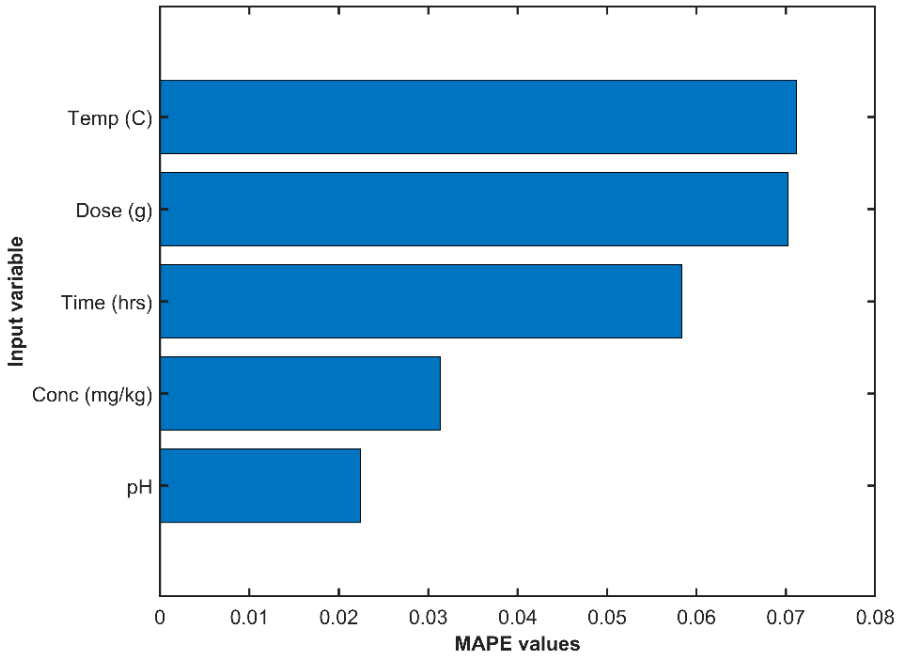

Figure 5. MAPE Values for the Inputs.

3. Results and Discussion

Table 2 compares the predicted values of lindane removal efficiency under optimal conditions for each developed model with the experimentally measured values of lindane removal efficiency. The training records are between 1 and 38, and the remaining records were used for testing the model. The standard deviations (SD) were computed for each data set and applied to both the experimental and the predicted values. The ANN-predicted values were found to be much closer to the experimental values. There was very little difference between the two of them, which was mirrored by the fact that there was minimal variation in the ANN SD values [37].

Table 2. Experiment and predicted removal efficiency for all datasets with their standard deviation.

SN	Dose (g)	pH	Conc (mg/kg)	Time (hrs)	Temp (C)	Exp Values (%)	ANN Predicted Values (%)	LN Predicted Values (%)	SD ANN	SD LN
1	50	7	1	24	24	43.492	45.314	49.145	1.288	3.998
2	100	7	1	24	24	59.058	57.837	55.807	0.864	2.299
3	300	7	1	24	24	80.194	80.064	82.455	0.092	1.599
4	150	2	1	24	24	65.838	65.846	64.769	0.006	0.756
5	150	4	1	24	24	65.272	65.258	63.849	0.010	1.006
6	150	7	1	24	24	63.319	67.944	62.469	3.271	0.601
7	150	10	1	24	24	64.440	64.233	61.090	0.146	2.369
8	150	7	0.5	1	24	54.100	56.122	61.136	1.430	4.975
9	150	7	0.5	6	24	62.778	61.306	61.235	1.041	1.091
10	150	7	0.5	16	24	68.424	66.077	61.434	1.660	4.943
11	150	7	0.5	24	24	64.910	65.815	61.593	0.640	2.346
12	150	7	0.5	48	24	52.710	54.430	62.070	1.217	6.618
13	150	7	0.5	96	24	62.973	62.444	63.023	0.374	0.036
14	150	7	0.75	1	24	55.639	57.167	61.574	1.081	4.197
15	150	7	0.75	2	24	59.529	58.296	61.594	0.872	1.460
16	150	7	0.75	16	24	69.869	66.803	61.872	2.168	5.655
17	150	7	0.75	24	24	69.594	67.018	62.031	1.821	5.348
18	150	7	0.75	48	24	57.622	56.045	62.508	1.115	3.455
19	150	7	1	1	24	57.368	58.191	62.012	0.582	3.284
20	150	7	1	2	24	60.344	59.297	62.032	0.740	1.194
21	150	7	1	6	24	63.954	63.022	62.112	0.659	1.303
22	150	7	1	24	24	67.670	67.944	62.469	0.194	3.677
23	150	7	1	48	24	57.475	58.079	62.946	0.427	3.869
24	150	7	1	96	24	63.085	63.651	63.900	0.400	0.576
25	150	7	1.5	2	24	60.806	60.600	62.909	0.146	1.487
26	150	7	1.5	6	24	64.064	64.133	62.988	0.049	0.761
27	150	7	1.5	16	24	66.922	68.224	63.187	0.921	2.641
28	150	7	1.5	48	24	64.006	63.077	63.823	0.657	0.129
29	150	7	1.5	96	24	63.745	64.878	64.777	0.801	0.729
30	150	7	2	1	24	57.974	58.190	63.766	0.152	4.095
31	150	7	2	6	24	61.884	61.914	63.865	0.021	1.401
32	150	7	2	16	24	66.955	65.526	64.064	1.011	2.044
33	150	7	2	24	24	65.519	66.774	64.223	0.887	0.917
34	150	7	2	48	24	64.326	64.511	64.700	0.130	0.264
35	150	7	2	96	24	67.331	66.091	65.653	0.876	1.186
36	150	7	1	24	24	66.404	67.944	62.469	1.089	2.782
37	150	7	1	24	30	59.879	61.858	60.207	1.399	0.232
38	150	7	1	24	40	56.558	56.178	56.435	0.269	0.087
39	150	7	1	24	24	65.206	67.944	62.469	1.936	1.935
40	200	7	1	24	24	74.010	74.979	69.131	0.685	3.450
41	150	8	1	24	24	65.392	66.234	62.009	0.596	2.392
42	150	7	0.5	2	24	56.353	57.256	61.156	0.639	3.396
43	150	7	0.75	6	24	65.078	62.206	61.673	2.031	2.407
44	150	7	0.75	96	24	65.093	63.045	63.462	1.448	1.154
45	150	7	1	16	24	67.294	67.389	62.310	0.067	3.524
46	150	7	1.5	1	24	55.645	59.504	62.889	2.729	5.122
47	150	7	1.5	24	24	64.514	69.205	63.346	3.317	0.826
48	150	7	2	2	24	61.022	59.066	63.786	1.383	1.954
49	150	7	1	24	35	58.699	59.247	58.321	0.387	0.267

Therefore, it is evident in Table 2 that the developed ANN model performed better than the SR model for this application. Similarly, the results of the modeled and experimental values for the training dataset are displayed in Figure 6a. As the figure demonstrates, the ANN-predicted values coincided much better with the experimental values than the SR-predicted values. Overall, the correlation between the ANN-predicted and experimental values in most datasets shows that the model could accurately predict the experimental values. A linear curve was obtained when plotting the experimental data against the predicted values for the training dataset (Figure 7a) [38]. The average correlation coefficient (r) of the experimental and ANN predicted values were 96.9%, and of SR predicted value was 73.59%, which further confirms the power of our ANN model to predict removal efficiency values from experimental data accurately [39]. Previously, Tariq et al. reported similar performance when they used the ANN model for the adsorption of methylene blue

on zeolite [40]. In the same vein, Figure 6b shows the experimental and predicted values results for the testing data set. The figure shows how well the experimental values and the ANN-predicted values agreed. To determine the degree of association or correlation coefficient between the two sets of values, the ANN and SR predicted values obtained from the developed models for the testing datasets were also plotted against experimental values (Figure 7b). The testing dataset obtained a correlation coefficient of 89.9% for ANN and 67.75% for SR, which showed a stronger association between the actual and ANN-predicted values.

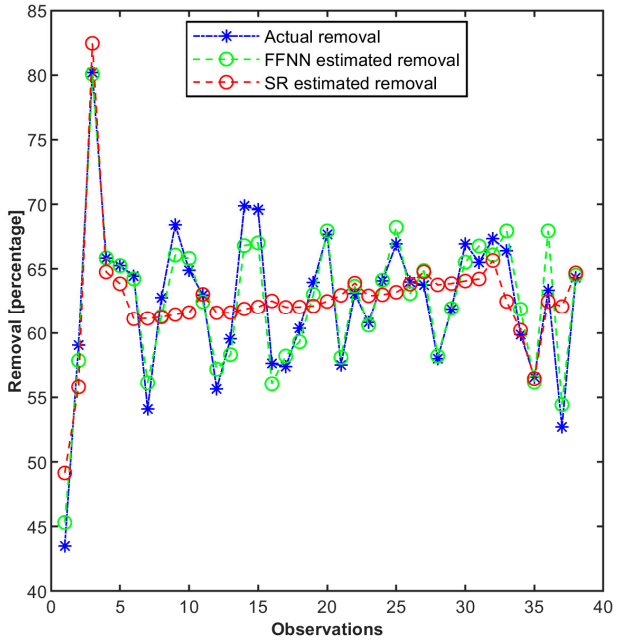

(**a**)

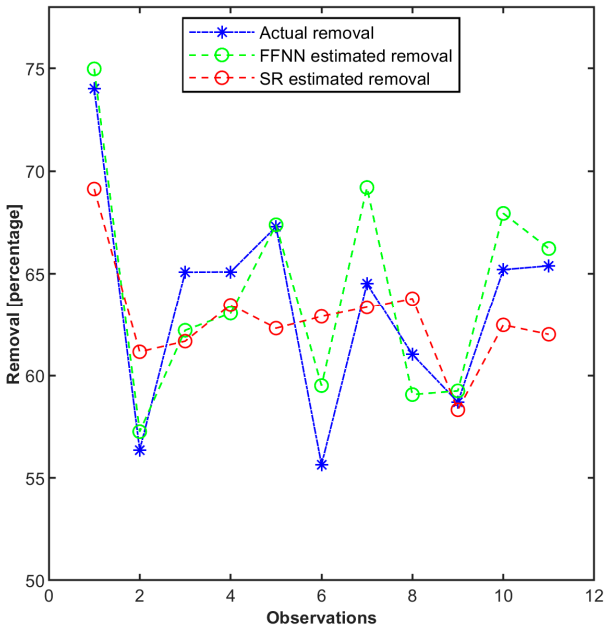

(**b**)

Figure 6. Line plots for the training dataset (**a**) and the testing dataset (**b**).

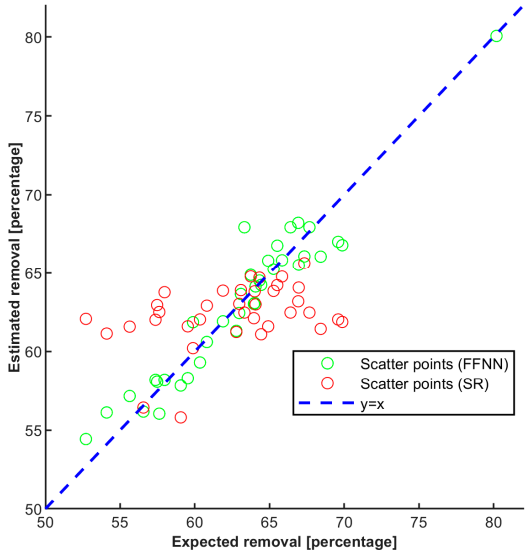

(**a**)

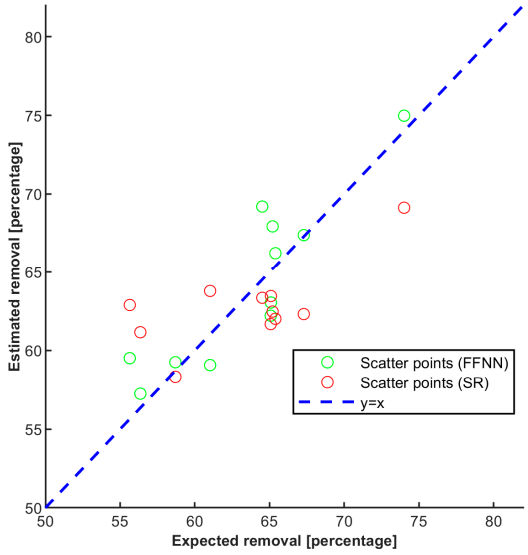

(**b**)

Figure 7. Scatter plots for the training dataset (**a**) and the testing dataset (**b**).

Additionally, RMSE, MAPE, and RSR are tools used to evaluate the error between the modeled values and experimental values. Lower RMSE, MAPE, and RSR values indicate a better model [41]. In contrast, the R^2 and WIA values vary from '0' to '1', where the number '1' indicates a perfect match between the actual and the estimated variables, whereas the number' 0' exhibits the output variables cannot be estimated from the given input variables. Besides, the ideal value of PBIAS is 0.0, which is a perfect match between the estimated and the actual variables. However, positive and negative values of PBIAS refer to underestimation and overestimation of the estimated outputs, respectively [42–46].

Table 3 presents the performance measuring parameters. RMSE, MAPE, and RSR represent a measure of the variances between values predicted by a model. The difference between experimental values and predicted values increases as the values rise. The ANN model's RMSE values for the training and testing datasets were 1.482 and 2.402, respectively, which were significantly lower compared to the SR model's RMSE values of 4.035 and 3.890 for training and testing, respectively. This was the conclusion of Altowayti et al.

when they used ANN to study the adsorptive removal of arsenic [47]. Additionally, it was noted that the ANN model's MAPE values for the training and testing datasets, which were 0.018 and 0.031, respectively, were significantly lower than the SR model's MAPE values, as shown in Table 3 and presented in Figure 8. Likewise, the RSR and PBIAS values are low for both training and testing datasets, indicating the developed model's strength. On the other hand, the R^2 and WIA values are more than 0.90 for both datasets, which also testify to the efficacy of the developed ANN model. Furthermore, the equation generated from the developed ANN model will allow us to vary several parameters simultaneously, which was hitherto difficult with OVAT-based experiments [41]. Therefore, the multivariate/inter-parametric interactions between the physico-chemical factors that contribute to the adsorptive absorption of pollutants in a synergistic and non-interactive manner can be examined. As seen in Figure 8, the ANN model arguably demonstrates superior performance to the SR model across the board in terms of all of the performance measuring parameters considered in this study.

Table 3. Performance measuring parameters.

Models	Class	RMSE	MAPE	RSR	R^2	WIA	PBIAS
ANN	Training Data	1.482	0.018	0.249	0.969	0.985	−0.087
	Testing Data	2.402	0.031	0.477	0.900	0.943	−1.113
SR	Training Data	4.035	0.052	0.677	0.736	0.885	0.541
	Testing Data	3.891	0.054	0.772	0.678	0.851	0.404

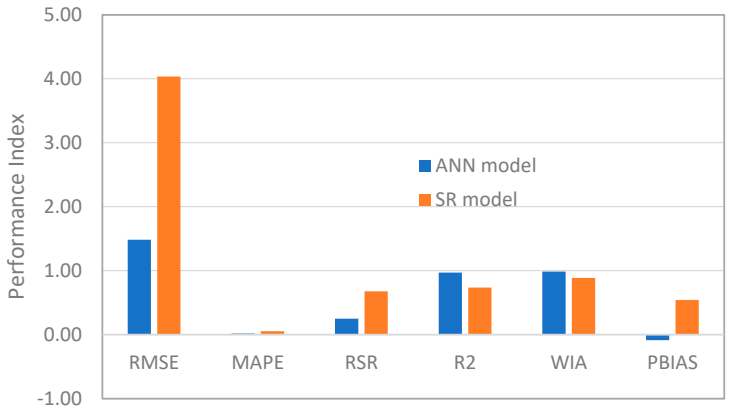

(**a**)

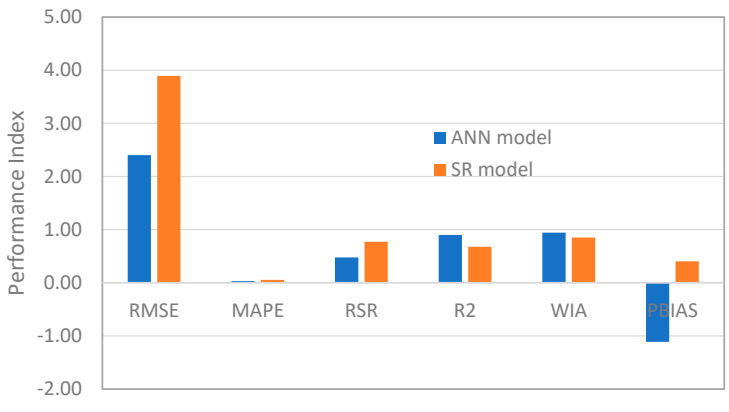

(**b**)

Figure 8. Performance measuring parameters for ANN and SR models for (**a**) Training dataset, (**b**) Testing dataset.

4. Conclusions

In this article, the ANN and SR models were proposed for multivariate calibration and analysis using the experimental data obtained from the OVAT experimentation. It was observed that the ANN was the better model for this application after comparing the performance of the two models. For each dataset, the standard deviations were calculated and applied to the experimental and the predicted values. The experimental and ANN-predicted values were discovered to be very close. A linear curve was produced when the experimental data were plotted against predicted values for the training dataset. The correlation coefficient, R^2, between experimental and ANN predicted values was 96.9%, whereas the correlation coefficient between experimental and SR predicted values was 73.59% for the training dataset. This further supports the ability of our ANN model to predict lindane removal with accuracy. The computed correlation coefficients for the testing dataset—89.9% for ANN and 67.75% for SR—showed a stronger correlation between the actual and ANN predicted values. The RMSE values for the training and testing datasets for the ANN model were 1.482 and 2.402, respectively, which were noticeably lower than the corresponding SR model RMSE values of 4.035 and 3.890. It was also found that the MAPE values for the training and testing datasets for the ANN model, which were 0.018 and 0.031, respectively, were noticeably lower than those for the SR model. The RSR and PBIAS values, which represent the strength of the developed model, are also low for both the training and testing datasets. However, the R^2 and WIA values are higher than 0.90 for both datasets, which further attests to the effectiveness of the developed ANN model. Therefore, it is believed that the overhead expenses related to the water treatment process are expected to decrease due to the application of our developed ANN model. The application will lower the cost of eliminating several inorganic and organic contaminants from the contaminated water, including lindane, and will optimize the use of chemicals.

Author Contributions: Conceptualization, A.A.A., M.S., M.K.N. and S.M.R.; methodology, M.K.N. and M.S.; software, M.S. and A.A.A.; formal analysis, M.S. and S.M.R.; resources, M.K.I. and M.M.I.; data curation, M.S. and M.M.R.; writing—original draft preparation, A.A.A., M.S. and M.M.R., writing—review and editing, M.M.R., A.R., M.K.N., S.M.R. and A.A.A.; supervision, M.K.N. and M.S.; project administration, M.S. and M.M.R.; funding acquisition, M.M.R. All authors have read and agreed to the published version of the manuscript.

Funding: This research was funded by the Deanship of Scientific Research at King Faisal University (KFU), Al-Ahsa 31982, Saudi Arabia, through Project No. GRANT 3415.

Institutional Review Board Statement: Not applicable.

Informed Consent Statement: Not applicable.

Data Availability Statement: The data that support the findings of this study are available from the corresponding authors, M.M.R. (mrahman@kfu.edu.sa) and M.S. (shafiullah@kfupm.edu.sa), upon reasonable request.

Acknowledgments: The authors acknowledge the support received from King Faisal University (KFU) and King Fahd University of Petroleum & Minerals (KFUPM), Saudi Arabia.

Conflicts of Interest: The authors declare no conflict of interest.

References

1. Zhang, S.; Liu, Z.; Li, S.; Zhang, S.; Fu, H.; Tu, X.; Xu, W.; Shen, X.; Yan, K.; Gan, P.; et al. Remediation of Lindane Contaminated Soil by Fluidization-like Dielectric Barrier Discharge. *J. Hazard. Mater.* **2023**, *443*, 130164. [CrossRef] [PubMed]
2. Yang, X.; Huang, X.; Cheng, J.; Cheng, Z.; Yang, Q.; Hu, L.; Xu, J.; He, Y. Diversity-Triggered Bottom-up Trophic Interactions Impair Key Soil Functions under Lindane Pollution Stress. *Environ. Pollut.* **2022**, *314*, 120293. [CrossRef] [PubMed]
3. Pannu, R.; Kumar, D. Biodegradation of Lindane (γ-Hexachlorocyclohexane) and Other Isomers by Bacillus Subtilis Strain Mz-13i. *Biocatal. Agric. Biotechnol.* **2023**, *48*, 102630. [CrossRef]
4. Khan, S.; He, X.; Khan, J.A.; Khan, H.M.; Boccelli, D.L.; Dionysiou, D.D. Kinetics and Mechanism of Sulfate Radical- and Hydroxyl Radical-Induced Degradation of Highly Chlorinated Pesticide Lindane in UV/Peroxymonosulfate System. *Chem. Eng. J.* **2017**, *318*, 135–142. [CrossRef]

5. Vidal, J.; Carvela, M.; Saez, C.; Cañizares, P.; Navarro, V.; Salazar, R.; Rodrigo, M.A. Testing Different Strategies for the Remediation of Soils Polluted with Lindane. *Chem. Eng. J.* **2020**, *381*, 122674. [CrossRef]
6. Pant, N.; Shukla, M.; Upadhyay, A.D.; Chaturvedi, P.K.; Saxena, D.K.; Gupta, Y.K. Association between Environmental Exposure to p, P′-DDE and Lindane and Semen Quality. *Environ. Sci. Pollut. Res.* **2014**, *21*, 11009–11016. [CrossRef]
7. Raimondo, E.E.; Saez, J.M.; Aparicio, J.D.; Fuentes, M.S.; Benimeli, C.S. Bioremediation of Lindane-Contaminated Soils by Combining of Bioaugmentation and Biostimulation: Effective Scaling-up from Microcosms to Mesocosms. *J. Environ. Manag.* **2020**, *276*, 111309. [CrossRef]
8. Akinpelu, A.A.; Nazal, M.K.; Abuzaid, N. Adsorptive Removal of Polycyclic Aromatic Hydrocarbons from Contaminated Water by Biomass from Dead Leaves of Halodule Uninervis: Kinetic and Thermodynamic Studies. *Biomass Convers. Biorefin.* **2021**, *in press*. [CrossRef]
9. Nath, B.K.; Chaliha, C.; Kalita, E. Iron Oxide Permeated Mesoporous Rice-Husk Nanobiochar (IPMN) Mediated Removal of Dissolved Arsenic (As): Chemometric Modelling and Adsorption Dynamics. *J. Environ. Manag.* **2019**, *246*, 397–409. [CrossRef]
10. Akbari, M.; Asadi, P.; Aliha, M.R.M.; Berto, F. Modeling and Optimization of Process Parameters of the Piston Alloy-Based Composite Produced by Fsp Using Response Surface Methodology. *Surf. Rev. Lett.* **2023**, *30*, 2350041. [CrossRef]
11. Asfaram, A.; Ghaedi, M.; Ghezelbash, R. Biosorption of Zn^{2+}, Ni^{2+} and Co^{2+} from Water Samples onto Yarrowia Lipolytica ISF7 Using a Response Surface Methodology, and Analyzed by Inductively Coupled Plasma Optical Emission Spectrometry (ICP-OES). *RSC Adv.* **2016**, *6*, 23599–23610. [CrossRef]
12. Alam, G.; Ihsanullah, I.; Naushad, M.; Sillanpää, M. Applications of Artificial Intelligence in Water Treatment for Optimization and Automation of Adsorption Processes: Recent Advances and Prospects. *Chem. Eng. J.* **2022**, *427*, 130011. [CrossRef]
13. Shafiullah, M.; Abido, M.A.; Al-Mohammed, A.H. Intelligent Fault Diagnosis for Distribution Grid Considering Renewable Energy Intermittency. *Neural Comput. Appl.* **2022**, *34*, 16473–16492. [CrossRef]
14. Ahmad, S.; Shafiullah, M.; Ahmed, C.B.; Alowaifeer, M. A Review of Microgrid Energy Management and Control Strategies. *IEEE Access* **2023**, *11*, 21729–21757. [CrossRef]
15. Asadi, P.; Aliha, M.R.M.; Akbari, M.; Imani, D.M.; Berto, F. Multivariate Optimization of Mechanical and Microstructural Properties of Welded Joints by FSW Method. *Eng. Fail. Anal.* **2022**, *140*, 106528. [CrossRef]
16. Breaux, H.J. *On Stepwise Multiple Linear Regression*; Army Ballistic Research Lab Aberdeen Proving Ground MD: Aberdeen, UK, 1967.
17. Liu, W.-J.; Niu, X.-J.; Yang, N.; Tan, Y.-S.; Qiao, Y.; Liu, C.-F.; Wu, K.; Li, Q.-B.; Hu, Y. Prediction Model of Concrete Initial Setting Time Based on Stepwise Regression Analysis. *Materials* **2021**, *14*, 3201. [CrossRef]
18. Wang, M.; Wright, J.; Brownlee, A.; Buswell, R. A Comparison of Approaches to Stepwise Regression on Variables Sensitivities in Building Simulation and Analysis. *Energy Build.* **2016**, *127*, 313–326. [CrossRef]
19. Mundry, R.; Nunn, C.L. Stepwise Model Fitting and Statistical Inference: Turning Noise into Signal Pollution. *Am. Nat.* **2009**, *173*, 119–123. [CrossRef] [PubMed]
20. Ali, Y.; Qin, A.; Aatif, H.M.; Ijaz, M.; Khan, A.A.; Ahmad, S.; Shahzad, U.; Yasin, M.; Rahman, S.U. A Stepwise Multiple Regression Model to Predict Fusarium Wilt in Lentil. *Meteorol. Appl.* **2022**, *29*, e2088. [CrossRef]
21. Loftus, J.R.; Taylor, J.E. A Significance Test for Forward Stepwise Model Selection. Available online: https://arxiv.org/abs/1405.3920 (accessed on 13 April 2023).
22. Krogh, A. What Are Artificial Neural Networks? *Nat. Biotechnol.* **2008**, *26*, 195–197. [CrossRef]
23. Ali, A.; Almutairi, K.; Malik, M.Z.; Irshad, K.; Tirth, V.; Algarni, S.; Zahir, M.H.; Islam, S.; Shafiullah, M.; Shukla, N.K. Review of Online and Soft Computing Maximum Power Point Tracking Techniques under Non-Uniform Solar Irradiation Conditions. *Energies* **2020**, *13*, 3256. [CrossRef]
24. Świetlicka, I.; Sujak, A.; Muszyński, S.; Świetlicki, M. The Application of Artificial Neural Networks to the Problem of Reservoir Classification and Land Use Determination on the Basis of Water Sediment Composition. *Ecol. Indic.* **2017**, *72*, 759–765. [CrossRef]
25. Rahman, S.M.; Khondaker, A.N.; Hossain, M.I.; Shafiullah, M.; Hasan, M.A. Neurogenetic Modeling of Energy Demand in the United Arab Emirates, Saudi Arabia, and Qatar. *Environ. Prog. Sustain. Energy* **2017**, *36*, 1208–1216. [CrossRef]
26. Ismail Hossain, M.; Shafiullah, M.; Abido, M. Induction Motor Speed Control Employing LM-NN Based Adaptive PI Controller. In Proceedings of the 18th International Conference on Renewable Energies and Power Quality (ICREPQ'20), Granada, Spain, 1–3 April 2020; Volume 18, pp. 97–102.
27. Haykin, S. *Neural Networks and Learning Machines*, 3rd ed.; Pearson Education, Inc.: Upper Saddle River, NJ, USA, 2009.
28. Aljohani, A.; Aljurbua, A.; Shafiullah, M.; Abido, M.A. Smart Fault Detection and Classification for Distribution Grid Hybridizing ST and MLP-NN. In Proceedings of the 2018 15th International Multi-Conference on Systems, Signals & Devices (SSD), Yasmine Hammamet, Tunisia, 19–22 March 2018; pp. 1–5.
29. Shafiullah, M.; Abido, M.A. S-Transform Based FFNN Approach for Distribution Grids Fault Detection and Classification. *IEEE Access* **2018**, *6*, 8080–8088. [CrossRef]
30. Tien Bui, D.; Tuan, T.A.; Klempe, H.; Pradhan, B.; Revhaug, I. Spatial Prediction Models for Shallow Landslide Hazards: A Comparative Assessment of the Efficacy of Support Vector Machines, Artificial Neural Networks, Kernel Logistic Regression, and Logistic Model Tree. *Landslides* **2016**, *13*, 361–378. [CrossRef]
31. Rana, M.J.; Shahriar, M.S.; Shafiullah, M. Levenberg–Marquardt Neural Network to Estimate UPFC-Coordinated PSS Parameters to Enhance Power System Stability. *Neural Comput. Appl.* **2019**, *31*, 1237–1248. [CrossRef]

32. Shafiullah, M.; Khan, M.A.M.; Ahmed, S.D. PQ Disturbance Detection and Classification Combining Advanced Signal Processing and Machine Learning Tools. In *Power Quality in Modern Power Systems*; Sanjeevikumar, P., Sharmeela, C., Holm-Nielsen, J.B., Sivaraman, P., Eds.; Academic Press: Cambridge, MA, USA, 2021; pp. 311–335.
33. Huang, G.-B.; Zhou, H.; Ding, X.; Zhang, R. Extreme Learning Machine for Regression and Multiclass Classification. *IEEE Trans. Syst. Man. Cybern. B Cybern.* **2012**, *42*, 513–529. [CrossRef] [PubMed]
34. Liu, H.; Lang, B. Machine Learning and Deep Learning Methods for Intrusion Detection Systems: A Survey. *Appl. Sci.* **2019**, *9*, 4396. [CrossRef]
35. Cecati, C.; Kolbusz, J.; Rozycki, P.; Siano, P.; Wilamowski, B.M. A Novel RBF Training Algorithm for Short-Term Electric Load Forecasting and Comparative Studies. *IEEE Trans. Ind. Electron.* **2015**, *62*, 6519–6529. [CrossRef]
36. Vinayagam, R.; Dave, N.; Varadavenkatesan, T.; Rajamohan, N.; Sillanpää, M.; Nadda, A.K.; Govarthanan, M.; Selvaraj, R. Artificial Neural Network and Statistical Modelling of Biosorptive Removal of Hexavalent Chromium Using Macroalgal Spent Biomass. *Chemosphere* **2022**, *296*, 133965. [CrossRef]
37. Karaman, C.; Karaman, O.; Show, P.L.; Karimi-Maleh, H.; Zare, N. Congo Red Dye Removal from Aqueous Environment by Cationic Surfactant Modified-Biomass Derived Carbon: Equilibrium, Kinetic, and Thermodynamic Modeling, and Forecasting via Artificial Neural Network Approach. *Chemosphere* **2022**, *290*, 133346. [CrossRef]
38. Gadekar, M.R.; Ahammed, M.M. Modelling Dye Removal by Adsorption onto Water Treatment Residuals Using Combined Response Surface Methodology-Artificial Neural Network Approach. *J. Environ. Manag.* **2019**, *231*, 241–248. [CrossRef]
39. Sarafraz-Yazdi Ac, A.; Khaleghi-Miran, S.-H.; Es 'haghi Bc, Z. Comparative Study of Direct Immersion and Headspace Single Drop Microextraction Techniques for BTEX Determination in Water Samples Using GC-FID. *Intern. J. Environ. Anal. Chem.* **2010**, *90*, 14–15. [CrossRef]
40. Tariq, R.; Abatal, M.; Bassam, A. Computational Intelligence for Empirical Modeling and Optimization of Methylene Blue Adsorption Phenomena Using Available Local Zeolites and Clay of Morocco. *J. Clean. Prod.* **2022**, *370*, 133517. [CrossRef]
41. Igwegbe, C.A.; Mohmmadi, L.; Ahmadi, S.; Rahdar, A.; Khadkhodaiy, D.; Dehghani, R.; Rahdar, S. Modeling of Adsorption of Methylene Blue Dye on Ho-$CaWO_4$ Nanoparticles Using Response Surface Methodology (RSM) and Artificial Neural Network (ANN) Techniques. *MethodsX* **2019**, *6*, 1779–1797. [CrossRef] [PubMed]
42. Akinpelu, A.A.; Ali, M.E.; Owolabi, T.O.; Johan, M.R.; Saidur, R.; Olatunji, S.O.; Chowdbury, Z. A Support Vector Regression Model for the Prediction of Total Polyaromatic Hydrocarbons in Soil: An Artificial Intelligent System for Mapping Environmental Pollution. *Neural Comput. Appl.* **2020**, *32*, 14899–14908. [CrossRef]
43. Lewis, C.D. *Industrial and Business Forecasting Methods: A Practical Guide to Exponential Smoothing and Curve Fitting*; Butterworth Scientific: San Diego, CA, USA, 1982; ISBN 0408005599.
44. Shafiullah, M.; Abido, M.A.; Al-Mohammed, A.H. *Power System Fault Diagnosis: A Wide Area Measurement Based Intelligent Approach*, 1st ed.; Elsevier: Amsterdam, The Netherlands, 2022; ISBN 9780323884303.
45. Moriasi, D.; Arnold, J.; Liew, M. Van Model Evaluation Guidelines for Systematic Quantification of Accuracy in Watershed Simulations. *Trans. ASABE* **2007**, *50*, 885–900. [CrossRef]
46. Willmott, C.J.; Robeson, S.M.; Matsuura, K. A Refined Index of Model Performance. *Int. J. Climatol.* **2012**, *32*, 2088–2094. [CrossRef]
47. Altowayti, W.A.H.; Algaifi, H.A.; Bakar, S.A.; Shahir, S. The Adsorptive Removal of as (III) Using Biomass of Arsenic Resistant Bacillus Thuringiensis Strain WS3: Characteristics and Modelling Studies. *Ecotoxicol. Environ. Saf.* **2019**, *172*, 176–185. [CrossRef]

Disclaimer/Publisher's Note: The statements, opinions and data contained in all publications are solely those of the individual author(s) and contributor(s) and not of MDPI and/or the editor(s). MDPI and/or the editor(s) disclaim responsibility for any injury to people or property resulting from any ideas, methods, instructions or products referred to in the content.